

UNIVERSITY OF LATVIA
FACULTY OF PHYSICS AND MATHEMATICS



Valdis Korsaks

LUMINESCENCE PROCESSES IN DIFFERENT
STRUCTURED BORON NITRIDE MATERIALS

Summary of Doctoral Thesis

Promotion to the Degree of Doctor of Physics

Subbranch: Solid State Physics

RIGA 2012

The dissertation work was carried out at the Institute of Solid State Physics, University of Latvia, in the time period from year 2007 to 2011.

Type of work: Dissertation.

Scientific advisor:

Dr. habil. phys. **Baiba Bērziņa**

Institute of Solid State Physics, University of Latvia

Dissertation Reviewers:

Dr. habil. phys. **Donāts Millers**, Institute of Solid State Physics, University of Latvia

Dr. habil. phys. **Uldis Rogulis**, Institute of Solid State Physics, University of Latvia

Dr. phys. **Marina Popova**, RAS, Institute for Spectroscopy, Russia

The dissertation defence will take place in the open session of the Physics, astronomy and mechanics dissertation commission of the University of Latvia to be held on April 26, 2012, at 16:00 in the conference hall of the Institute of Solid State Physics at Ķengaraga Street 8.

The thesis is available at the Library of the University of Latvia Multi-branched Library: Computer Science, Law and Theology, Raiņa Blvd. 19.

The dissertation was supported by European Social fund

Chairperson of specialized dissertation commission of University of Latvia in Physics, astronomy and mechanics: *Dr. habil. phys. prof.* **Ivars Tāle**

© Valdis Korsaks, 2011

© University of Latvia, 2011



**LATVIJAS
UNIVERSITĀTE**
ANNO 1919

IEGULDĪJUMS TAVĀ NĀKOTNĒ

Table of contents

Summary	4
1. Introduction	5
1.1. Timeliness and motivation of the work	5
1.2. The aim of this work.....	6
1.3. Scientific novelty.....	6
1.4. Author's contribution	7
2. Physical background.....	7
2.1. Morphology and energy band structure of BN.....	7
2.1.1. Hexagonal boron nitride (hBN).....	7
2.1.2. Hexagonal boron nitride nanotubes (BNNTs).....	8
2.1.3. Defects in hBN and BNNTs	9
2.2. Spectral characterization of BN.....	9
2.2.1. Exciton luminescence in hBN and BNNTs	9
2.2.2. Defect luminescence in hBN and BNNTs materials	9
2.2.3. Phonon spectra of hBN and BNNTs.....	10
3. Samples under investigation.....	10
4. Experimental methods	11
5. Result analysis.....	12
5.1. Natural defects in hBN and BNNTs.....	12
5.2. Luminescence of natural defects in hBN and BNNTs	14
a) 320 nm luminescence	16
b) 400 nm luminescence	23
c) PL bands in 500 nm region.....	27
6. Conclusions	29
7. Thesis.....	31
8. References	32
9. List of publications	35
Acknowledgements	37

Summary

This work is devoted to studies of spectral properties of hexagonal boron nitride macro material– polycrystalline grain powder (hBN) and nano material – multiwall nanotubes (BNNTs). In the work it was found that in all studied materials photoluminescence spectra contain the same bands, the most intensive bands are located at 320 nm and 400 nm. It allows concluding that identical natural defects are generated in BN crystal lattice during synthesis process. They are characteristic both to macro and nano material and they are not affected by the size scale. It was found that 320 nm and 400 nm bands and their excitation bands have fine structure. The fulfilled IR absorption studies have shown that the fine structure is caused by optical phonons (LO and TO). It was observed that the mentioned luminescence bands are excited also by host lattice excitons, exciton energy being transferred to defects, exciting them and causing luminescence. The fulfilled spectral measurements allow determining luminescence mechanism for 320 nm and 400 nm bands in hBN and BNNTs. The main contribution to 320 nm luminescence is made by intracenter processes, when light absorption and emission occurs in one and the same impurity atom. The main contribution to 400 nm luminescence is made by recombination processes. Dependence of 400 nm luminescence intensity on oxygen concentration in ambient atmosphere observed for hBN and BNNTs allows proposing of this material for application as oxygen sensor.

1. Introduction

This Doctoral Thesis is devoted to study of spectral properties of prospective wide band material – boron nitride taken in the form of macrosized polycrystalline grains and multiwall nanotubes.

1.1. Timeliness and motivation of the work

In recent decades many world laboratories devote ever growing attention to creation of new materials with enhanced properties, which could be used for production of optoelectronic devices of new generation. The most suitable materials for this purpose are semiconductors with wide band gap E_g including group III nitrides and related materials. One of the most studied materials is graphite – a form of carbon. In the end of the last century it was found that it is possible to produce graphite nanostructures whose properties essentially differ from properties of macro size material. Application of nanomaterials in optoelectronics offers prospects of not only enhanced parameters but also reduced size of devices. The best known carbon nanostructures are singlewall and multiwall nanotubes (SWCNTs and MWCNTs) and graphen. In recent time carbon nanomaterials have found use not only in optoelectronics but also in medicine. For that reason different research centres synthesize more and more new C nanomaterials, which are being studied in numerous world laboratories and research centres.

It was found that hexagonal boron nitride (hBN) obtains properties, which are similar to those of graphite. This material similarly to graphite has layered hexagonal structure, where B and N atoms are connected with covalent bonds in hexagonal rings forming honeycomb layers, while adjacent layers are interconnected with much weaker van der Waals forces. Moreover, it is possible to produce also boron nitride nanostructures, among them singlewall and multiwall nanotubes (SWBNNTs and MWBNNTs) are the most prospective for practical application. BN and C nanotubes have many common useful properties such as high thermal conductivity, high melting point (above 2000 °C), durability and flexibility of nanotubes, unreactiveness with different gases, etc. BN and C nanotubes have different electrical properties: C nanotubes are conductors, while C nanotubes are dielectrics.

Similarity (as well as distinction) of the both mentioned materials has aroused great interest also in hBN. That is why this material is also intensively produced and studied in many world laboratories during last two decades. Potential application of this material to a great extent is determined by its optical properties, which in turn are determined not only by material structure but also by presence of defects. Therefore it is important to estimate the present material defects and their effect on properties of the material.

Spectral study is one of methods, which gives information about presence and properties of defects in the material. This method is chosen for fulfilment of the studies specified in the Doctoral Thesis. In the given work it is planned to study spectral properties of hBN macromaterial and nanomaterial - hBN un MWBNNTs, in order to elucidate the defect-induced processes in these materials, which determine

their potential application, and hence, in context of the above mentioned reasons, determine also **timeliness and motivation of this Doctoral thesis**.

1.2. The aim of this work

The aim of this work is to study spectral properties of hBN different macromaterial types (synthesized in the form polycrystalline grains by different methods and under different conditions) and nanomaterial (MWBNNNTs) in order to: 1) trace the light-induced processes in samples; 2) detect intrinsic luminescence defects present in a sample and the corresponding luminescence mechanisms; 3) elucidate mechanisms of energy transfer from the excited host lattice to defects; 4) elucidate processes of light-induced energy storage in the material; 5) find out how/if the above mentioned processes change with decrease of material size – with transition from macro- to nano- scale size; 6) estimate material properties and connect them with potential application.

1.3. Scientific novelty

In this work there have been obtained new experimental results, which allow elucidating of light-induced processes in BN material – both macrosized polycrystalline grains and multiwall nanotubes (BNNTs), as well as comparing these processes in both mentioned material types.

1. For the first time the 320 nm luminescence, which is observed both in hBN grains and BN nanotubes, was studied using a complex of spectral methods (including measurements of photoluminescence and its excitation spectra in the wide temperature region from 8 K up to room temperature, optically stimulated luminescence (OSL) and thermoluminescence (TL), as well as luminescence kinetics and infrared light absorption). The results obtained are in good agreement with literature data. They allow identification of the 320 nm luminescence mechanism as intracenter luminescence, where optical excitation and the following emission occurs in one and the same atom. The 320 nm luminescence is caused also by energy transfer to luminescence center from excitons - the excited host lattice. There has been proposed an energy band/level diagram illustrating the mentioned processes. The obtained results indicate that the corresponding luminescence centres can be located in the bulk of the material. The proposed model gives reasonable interpretation of the observed experimental facts. Regrettably our fulfilled experiments do not allow precise identification of an atom, which forms the luminescence centre. Also literature data do not contain any proved identification of this defect, except for mentioning that the 320 nm luminescence band could be caused by C or O natural defects.

2. For the first time the 400 nm luminescence was studied using the above mentioned spectral methods. The phonon induced fine structure has been found in the 400 nm luminescence and corresponding excitation spectra. The experimental results allow concluding that 400 nm luminescence is caused by recombination processes. It means that there are several defects participating in the luminescence process, which are located in different sites of crystalline lattice. The 400 nm luminescence is caused not only by direct excitation but also by energy transfer from host lattice excitations –

excitons. It has been found that 400 nm luminescence is affected by environmental oxygen. Under influence of oxygen the intensity of 400 nm luminescence decreases. It allows concluding that the 400 nm luminescence is caused mainly by defects on surface or in its close vicinity. For this case also an energy band/level diagram is proposed, illustrating light-induced processes in a sample. Unfortunately is not possible to identify precisely the defects forming recombination luminescence centre. Presumably these defects may be connected with oxygen atoms and host vacancies.

3. For the first time it was stated that the 320 nm and 400 nm luminescence is observed both in hBN and in BNNTs and their properties are not affected by material size.

4. There is proposed a new application of hBN – a sensor for detection of oxygen concentration in gas mixtures.

1.4. Author's contribution

- The author has done a major work substantially redesigning and upgrading two experimental setups for spectral measurements. In the already existing experimental setups the light detecting systems were replaced, new electronic and mechanical units were constructed and installed, experiment control software was developed. The experimental setups were adapted for measurements at low temperatures and different gaseous media.
- The main part of the measurements was done by the author himself. The studies of boron nitride were started already in the author's Bachelor work and were continued in the Master work. The measurements undertaken in LU ISSP Laboratory of Wide Band Materials (photoluminescence, OSL and their characteristics) were done solely by the author. Particular measurements were done in other laboratories both in LU ISSP (studies of luminescence kinetics, impurity and structure identification by X ray fluorescence (XRF) and X ray diffraction (XRD) methods) and in foreign research centres (infrared light absorption – Frascati Research Center, Italy; TL measurements – Nice-Antipolis University, France) together with local scientists.
- Analysis of the obtained results was done discussing the results with colleagues, presenting them at seminars and local and international conferences.

2. Physical background

2.1. Morphology and energy band structure of BN

2.1.1. Hexagonal boron nitride (hBN)

Boron nitride (BN) is composed of group III element boron (B) and group V element nitrogen (N). There are known four stable lattice structures of BN: hexagonal (hBN), cubic (cBN), wurtzite (wBN) and rhombohedral (rBN) [1]. The given work is devoted to investigations of hexagonal BN, whose structure is similar to that of graphite (Fig. 2.1.1).

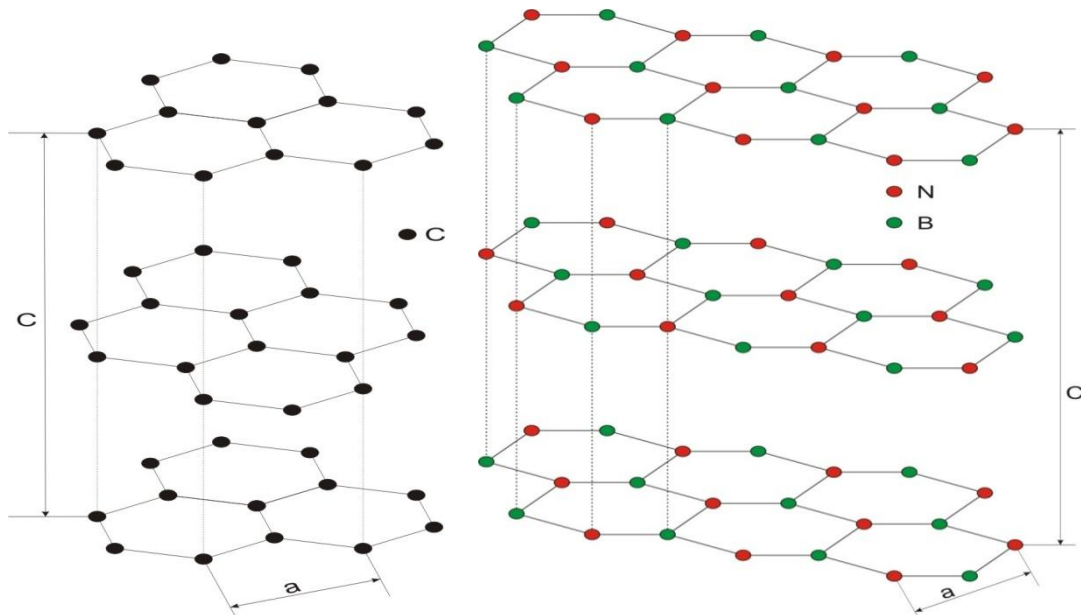


Fig. 2.1.1 Crystal lattice structure of graphite (left) and hBN (right) [2].

BN can be produced by different methods. hBN in powder form comprised of polycrystalline grains is synthesized by numerous methods, which are described in papers [3, 4, 5, 6, 7]. There are data found on hBN single crystal synthesis (Watanabe u.c. [8]). Structure of graphite and hBN are very similar, their lattice parameters a and c have only small differences. Graphite parameters are $a = 2,456 \text{ \AA}$, $c = 6,696 \text{ \AA}$ and hBN parameters are $a = 2,504 \text{ \AA}$, $c = 6,661 \text{ \AA}$. In hBN layers are bound by van-der-Waals forces, whereas B and N atoms located in one plane are tied with strong covalent bonds, the distance between adjacent atoms being $1,44 \text{ \AA}$ (sp^2 hybridization). Distance between layers in hBN is $c/2 = 3,33 \text{ \AA}$. There are free atom bonds on the edge of hBN crystal, which can attach other atoms or to form nanoarcs (singlewall or multiwall) by associating with free bonds from adjacent layers [9, 10]. Band gap of hBN is $\sim 6 \text{ eV}$, this material is thermally stable and chemically inert.

hBN can be practically applied in the following way. Due to laminated structure hBN is used as lubricant in broad temperature region. hBN is used also in optoelectronics and UV light emitters and laser materials (Watanabe and other papers [8]).

2.1.2. Hexagonal boron nitride nanotubes (BNNTs)

For the first time hexagonal boron nitride nanotubes were produced in 1995 [11]. They are similar to carbon nanotubes. BNNTs are produced by rolling up one or several hBN layers and forming correspondingly singlewall or multiwall nanotubes. Nanotubes have different diameter and length. They can have both open and closed end. Each nanotube has its characteristic chirality (armchair, zig-zag or chiral).

Today hBN nanotubes can be produced by different methods, obtaining any of the mentioned chirality types. These methods are similar to those of carbon nanotube production [11, 12, 13, 14, 15].

BNNTs is wide gap semiconductor ($E_g \sim 6 \text{ eV}$). Chirality type does not modify band gap [16, 17]. BNNTs is chemically and thermally stable material. BNNTs are more flexible and oxidation-stable compared to CNTs [18, 19].

BNNTs can be applied in polymer composite materials, glasses and ceramics, nano dielectrics and UV light emitters.

2.1.3. Defects in hBN and BNNTs

There are known numerous point defect types in hBN macromaterial and nanomaterial. They are host material atom vacancies (V_B , V_N , V_{3B+N} [20]); substituting defects B_N and N_B [21]; interstitial defects i_N and i_B . In this material F-center type defects can be produced comprised of 3 boron atoms and nitrogen vacancy with an attached electron $-3B+V_N+e^-$ [22, 23, 24]. Besides impurity defects are possible. Impurity defects in BN may be divided into two groups. 1) Intrinsic defects entering lattice during production process. They are: O; C; Si, and others. 2) Artificial defects: Eu, Ce, Ge, Mn and others [22, 25]. All these defects form their levels in host lattice band gap and are characterized by particular spectral properties. In hBN material there can be formed special defects (the so-called Stone-Walls defects) due to damage of hexagon cells. The damaged cell can contain 5 atoms (deficit) or 7, 8 and more atoms (surplus).

2.2. Spectral characterization of BN

Spectral properties of BN materials (macromaterials and nanomaterials) provide essential information about luminescence processes taking place in these objects. In BN luminescence is caused by excitons, intrinsic and artificial defects. The main investigations are made by Japanese, French, Australian, American and other groups of scientists.

2.2.1. Exciton luminescence in hBN and BNNTs

Some papers are devoted to photoluminescence and cathodoluminescence of hBN [26, 27, 28, 29, 30] and BNNTs [31, 32]. Strong UV luminescence is observed in single hBN crystals around 215 nm (5,76 eV), it is connected with luminescence of free excitons [33, 34, 35, 36]. In papers of K. Watanabe and other works emission of free excitons at 215 nm is observed together with emission of bound exciton at 227 nm (5,46 eV). Whereas in cathodoluminescence spectra of nanomaterials (multiwall nanotubes with diameter 50 nm) emission of free exciton is observed at 5,27 eV. Comparing exciton luminescence in hBN and BNNTs materials, it is seen that emission spectrum in nanomaterials is shifted by 500 meV to the long wavelength side [31]. Luminescence life time was measured in hBN: for free excitons is was 9 ps, and for bound excitons - 2,9 ns [33, 37]. Free excitons are ascribed to Frenkel type excitons with large binding energy $\sim 0,7$ eV [38, 39].

Exciton processes for boron nitride nanotubes of different tube diameter are being studied also theoretically [40, 41].

2.2.2. Defect luminescence in hBN and BNNTs materials

Defects potentially present in hBN were studied by EPR method [22, 23, 24]. A special attention was drawn to C impurity, which forms a definite level in energy band gap. However a direct evidence of C presence in the material was not found. Taniguchi and Watanabe have studied luminescence of hBN with different concentrations of oxygen and carbon impurities. They have found that intensity of the

320 nm emission band grows sufficiently with increase of O and C concentrations [33]. Usually researchers connect the 320 nm emission band with O or C impurities. In BNNTs materials this 320 nm PL emission band is also observed [32, 42] and similarly to hBN it is associated with O or C impurities, although no direct confirmation of this assumption was obtained.

Apart from the above mentioned 320 nm PL band also other PL bands are observed in hBN, they are described in papers [42, 43, 44, 45, 46, 47]. In turn Hua Chen et al. have observed the 400 nm band in BNNTs (with diameter 100 nm), which they did not identify, but proposed the material for application as a visible light emitter, because luminescence intensity is much stronger than in hBN [48].

For hBN and BNNTs materials rare earth elements luminescence is being studied: it is found that hBN has PL bands in visible spectral area around 560 nm, 470 nm and 410 nm, which are ascribed to Eu, Ce, and Ge impurities [49], whereas in BNNTs nanomaterial Eu impurity causes luminescence band at 500 nm and ytterbium (Yb) luminescence is observed at 573 nm and 483 nm [50].

In theoretical works there was studied O₂ adsorption in BNNTs material and its separation from nanotube surface. The processes are studied for perfect BNNT singlewall nanotubes (10, 0) and nanotubes with defects: V_N, V_B, vacancies and distorted host cells - Stone-Wallies defects. The obtained results imply that O₂ interaction with perfect BNNT nanotubes is very weak. In contrast in nanotubes containing V_N vacancies, O₂ is easily absorbed on nanotube surface, but in case of V_B vacancies and other defects O₂ is not observed [51].

2.2.3. Phonon spectra of hBN and BNNTs

Both experimental and theoretical studies of Raman and IR absorption spectra have been done for hBN material. Several phonon induced bands were found [52, 53, 54, 55]. Raman and IR absorption bands were observed at 200 meV, 170 meV, 100 meV and others, these coincide with theoretical calculations. Each observed band corresponds to a definite optical (LO, TO, ZO) or acoustic phonon type (LA, TA, ZA).

Raman and IR absorption measurements in BNNTs nanomaterial and theoretical calculations are reflected in papers [56, 57]. In IR absorption measurements of multiwall nanotubes bands are observed at 800 cm⁻¹, 1372 cm⁻¹ and 1540 cm⁻¹. The observed bands coincide with theoretical calculation results and characterize ZO, LO and TO optical phonons.

3. Samples under investigation

Two types of hBN macromaterial and two types of hBN nanomaterial were studied in this work; each material was produced by a particular method.

Macromaterials:

- a) **Sample A** – macromaterial - hBN powder synthesized by Aldrich Corp. It was obtained from Wake Forest University, USA (Department of Physics and Center for Nanotechnology and Molecular Materials, Wake Forest University). Grain size is around 3 μm ; purity of material is 99,5 %.
- b) **Sample B** - macromaterial hBN powder synthesized by Aldrich Corp. It was obtained from Belarus.

Nanomaterials

- a) **Sample C** - nanomaterial – multiwall nanotubes BNNTs is synthesized in Wake Forest University, USA, using macromaterial A as initial material. Sample contains multiwall nanotubes with diameter 5 nm - 30 nm. Besides the sample contains small amount of hBN particles remaining after synthesis.
- b) **Sample D** - BNNTs nanomaterial is synthesized in USA, NanoAmor. Corp., The sample contains multiwall BNNTs with diameter 40 nm - 100 nm. Purity of this sample is 99.5% (producer data).

4. Experimental methods

The following experimental methods were used in the given work.

Setup for photoluminescence (PL) and photoluminescence excitation (PLE) measurements.

There are two setups for luminescence measurements in Laboratory of Wide Band Gap Materials. These setups are meant for PL spectra measurements in spectral region 250 nm – 800 nm and PLE spectra measurements in 200 nm – 400 nm region; thermal region of measurements is 8K – 300 K. Sample luminescence is excited with light from a deuterium lamp (400 W) or YAG pulse laser RQSS 266 (CryLas GmbH) forth harmonic at 266 nm (4,66 eV). Exciting light and luminescence light is selected with monochromators MDR2, SPM2 and Andor SR-303i-B. Luminescence is detected with Andor CCD camera DV 420A-BU2 or Hamamatsu H7468-20 and H7468-03 detectors.

Setup for optically stimulated luminescence measurements.

OSL was studied using the modified setup for photoluminescence studies. First of all a sample is irradiated with the desired wavelength (deuterium lamp 400W). Optical stimulation is performed by laser KLM-H 650-40-5 with $\lambda = 650$ nm. Luminescence is detected by the above mentioned detectors.

Setups for thermoluminescence and IR absorption

TL measurements were fulfilled in Nice-Sophia Antipolis University, France, while IR absorption measurements were done in Frascati Research Centre, Italy, using there available equipment.

Measurements of X ray fluorescence spectra

A setup EAGLE III in ISSP Laboratory of Amorphous Material Spectroscopy was used for detection of impurity composition present in the samples. The setup consists of vacuum camera, Si detector with Be window and source of X rays.

Measurements of X ray diffraction spectra

Setup for X ray diffraction (XRD), which is available in ISSP Laboratory of Functional Material Physics and Application, was used for detection of samples structure and lattice constants. XRD powder diffractometer X'Pert PRO, PANalytical was used for measurements. The diffractometer is equipped with Cu anode electron lamp with characteristic wavelengths K-Alpha = 0,1540598 nm and K-Beta 0,1392250 nm. Ni filters were used for measurements. Interpretation of experimental results was done using data base „PDF-2” and software „UnitCell”.

Setups for luminescence decay time measurements

Luminescence decay time measurements were done using two setups. The first one, which is located in ISSP Laboratory of Solid State Radiation Physics, is meant for detection of decay times higher than 5 ns. The other one, which is available in ISSP Laboratory of Optical Spectroscopy, is used for measurements of short luminescence decay times < 5 ns.

- 1) On the first setup the sample was excited with YAG pulse laser RQSS266 (CryLas GmbH) forth harmonic at 266 nm (4,66 eV) with pulse length 5 ns. Luminescence kinetics was detected using phonon count detector H8259-02 (HAMAMATSU).
- 2) The second setup is equipped with Nd:YAG laser (PG401/SH, Ekspla), whose third harmonic with pulse duration 30 ps is used as a light source. The luminescence signal was analyzed with BRUKER Optics (250is/sm) monochromator and detected with C4334-01 (HAMAMATSU) camera.

5. Result analysis

This chapter gives review and analysis of the results obtained for hBN un BNNTs materials, including studies of photoluminescence and its excitation spectra at different temperatures, infrared (IR) absorption, thermoluminescence (TL), optically stimulated luminescence (OSL) and luminescence kinetics. This chapter shows a part of obtained spectra measured during elaboration of this work.

5.1. Natural defects in hBN and BNNTs

The samples under investigation were subjected to X ray diffraction measurements in order to determine crystal phase and lattice constants. The obtained

results are shown in Fig. 5.1. Characteristic maxima were detected for samples A and B, comparing their position with literature data [58] and PDF-2 data base it can be concluded that these samples belong to hexagonal phase. Sample D reveals also maxima, which are no relevant for hBN (marked with red points on the graph) and according to data base correspond to ZrO₂ [59].

In order to determine lattice constants for hBN material, X ray spectrum was analyzed using „UnitCell” software. The following values were obtained, well correlating with literature data: $a = 2.506 \text{ \AA}$ and $c = 6.660 \text{ \AA}$ [2].

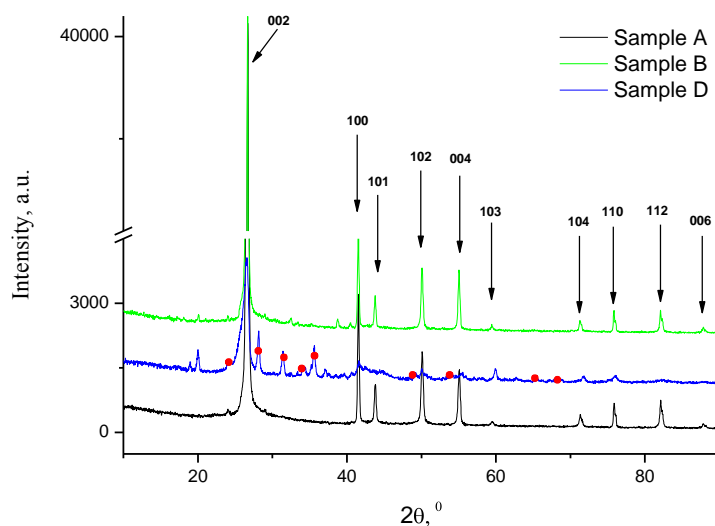


Fig. 5.1 X ray diffraction measurements for samples A, B, D. Arrows show maxima characteristic for hBN, red points mark maxima characteristic for ZrO₂.

Samples A and D were subjected to XRF measurements, in order to determine impurities present in these samples.

Summary of information on the samples used in this work is given in Table 1.

Table 1. Characteristics of investigated samples

Material	Sample label	Material size	Synthesis method	Impurities (XRD, XRF)	Lattice constants [2]	Producer
hBN	A	~3 μm	Unknown	C, O, P, Ca, Ti, Fe	$a = 2.506 \text{ \AA}$ $c = 6.660 \text{ \AA}$	Aldrich. Cor
hBN	B	~3 μm	Unknown	C, O, P, Ca, Ti, Fe	$a = 2.506 \text{ \AA}$ $c = 6.660 \text{ \AA}$	Aldrich, Cor.
BNNTs	C	5-30 nm (external diameter)	Arc discharge method	C, O, P, Ca, Ti, Fe	Unknown	WF University, ASV
BNNTs	D	40-100 nm (external diameter)	High temperature catalysis method	C, O, Si, Ca, Ti, Cr, Fe, Ni, Cu, Zr, ZrO ₂ , Y, Na, Al un Zn	Unknown	NanoAmor Cor. ASV

5.2. Luminescence of natural defects in hBN and BNNTs

In this work luminescence was studied for hBN materials of different structure, which were produced in different places using different methods. These materials include two types of hBN macrosize powders and two types of BNNTs nanomaterials (multiwall nanotubes). Luminescence spectra of these materials are complex; they contain several broad bands, which are characterized with fine structure.

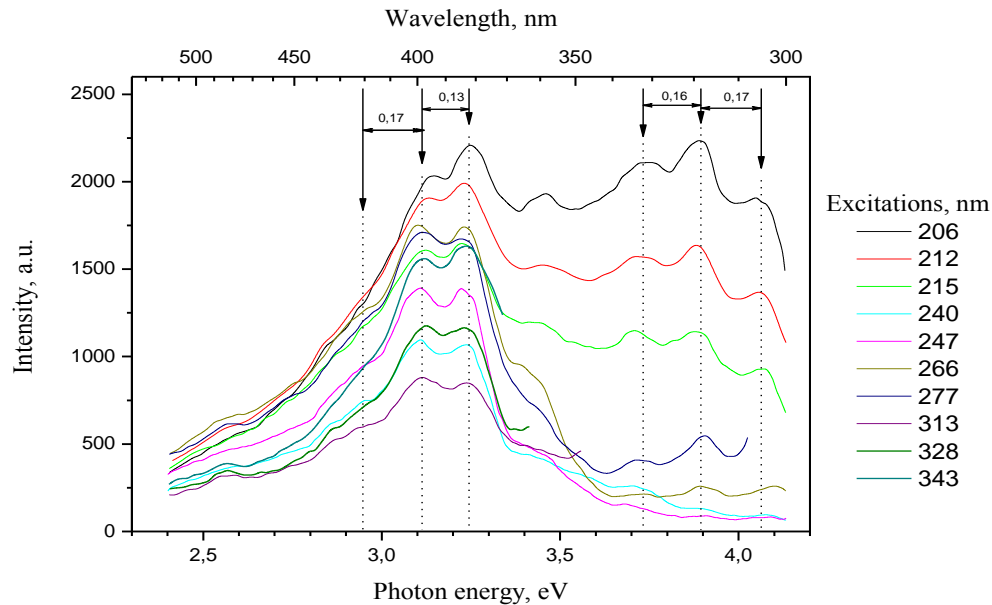


Fig. 5.2.1 PL spectra of h-BN (A) macromaterial at temperature 300 K. The spectra are measured using different excitation wavelength shown at the right.

Fig.5.2.1 shows luminescence spectra of sample A at 300 K. The most intensive luminescence is observed in the 300 - 400 nm spectral range. Two broad luminescence bands can be distinguished – those at 320 nm and 400 nm. (The bands are better distinguished using optimal observation conditions – excitation wavelength and temperature). Several weaker luminescence bands are observed in the longer wavelength part higher than 450 nm, their intensity grow at low temperatures. In this work the main attention is devoted to 320 nm and 400 nm luminescence. Both mentioned bands are observed in all studied materials – either macrosize or nanostructured. Ratio of two bands intensities is different in different materials, but position remains practically unchanged.

400 nm and 320 nm luminescence is excited by host free excitons and bound excitons (Fig.5.2.1 (A) and 5.2.2 (B)).

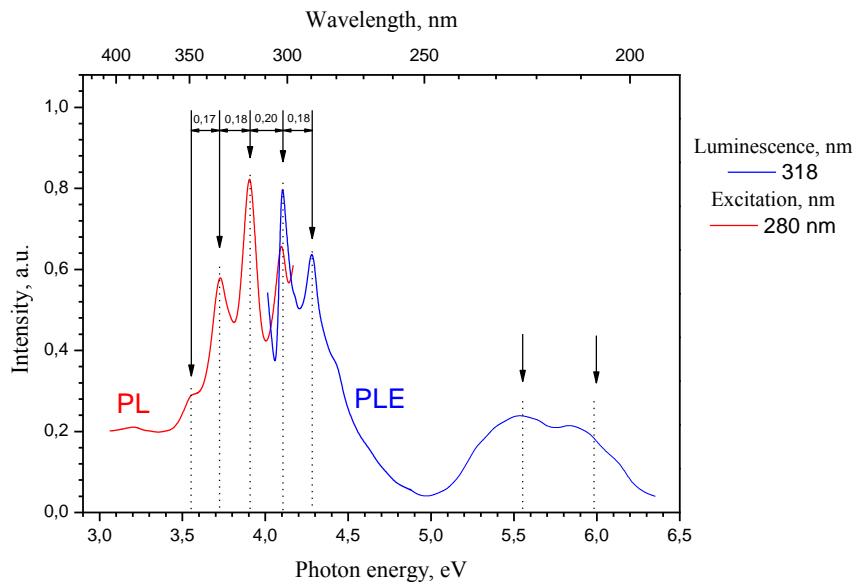


Fig. 5.2.2 PL and PLE spectra of hBN (sample B) at 80K.

Besides, each luminescence band has its own distinct excitation bands with energy below boron nitride energy band gap E_g , which correspond to defect absorption. 320 nm luminescence is excited in one band at 300 nm (see Fig. 5.2.2 (B)). 400 nm luminescence has two excitation bands at 265 nm and 345 nm (see Fig. 5.2.3 (A)).

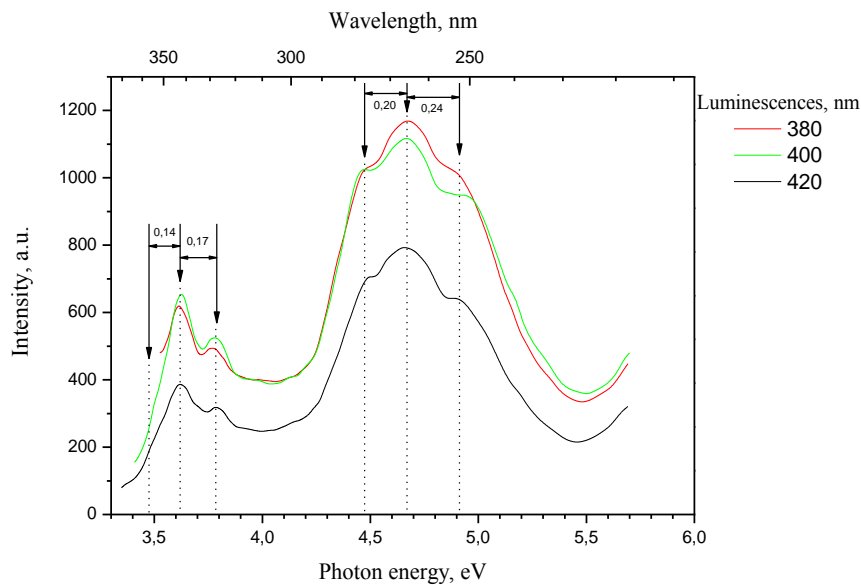


Fig. 5.2.3 PLE spectra of hBN (sample A) at temperature 300 K. Selected luminescence intervals I (± 6 nm) corresponding to excitation spectra are seen at right side.

Luminescence bands are connected with luminescence centres causing this emission. The concerned luminescence and excitation spectra allow concluding that there are two distinctive luminescence centres responsible for 320 nm and 400 nm

luminescence bands, because not only luminescence bands but also their absorption/excitation bands have different spectral position.

Comparison of 320 nm and 400 nm luminescence and its excitation spectra in boron nitride samples of different origin and size **allows concluding that:**

- Two types of natural defects forming luminescence centres, which are responsible for 320 nm and 400 nm emission, are characteristic for hexagonal boron nitride. Their presence is observed in all studied samples.
- In boron nitride macromaterial and nanomaterial position of the 320 nm and 400 nm luminescence bands and their excitation bands does not depend on material size. No regular spectral shift is observed comparing macromaterials and nanomaterials.
- Both in hBN macropowder and BNNTs host lattice excitation (excitons) energy is transferred to defects, which are responsible for 320 nm and 400 nm luminescence.

Photoluminescence bands 320 and 400 nm obtained in this work in hexagonal boron nitride are in good agreement with measurements of other authors who have used other methods apart from direct excitation of luminescence centres [31, 32, 42]. Other authors have studied mainly cathodoluminescence (320 nm band in paper [60], see Fig.3.2.2.1), as well as exciton excited luminescence. Photoluminescence spectra are seen in Wu et al. paper [42], where 320 nm band is well expressed; the 400 nm band with its fine structure is also seen but it is not discussed. The presence of the broad 400 nm band is seen also in Hua Chen paper [48].

More detailed analysis of 320 nm and 400 nm luminescence bands is given lower.

a) 320 nm luminescence

As it has been already mentioned, 320 nm luminescence is characteristic for different structures of hexagonal boron nitride; it is excited by both host excitons and defect absorption in 300 nm band. Let us analyse properties of this luminescence in details.

The broad 320 nm (3,87 eV) luminescence band in samples A, B, C, D was observed in PL spectra, measured both at room temperature (Fig. 5.2.1), and low temperatures [our papers 30, 61]. This band is complex and has at least 3 subbands at 305 nm (4,06 eV), 318 nm (3,89 eV) and 332 nm (3,73 eV). Separation between adjacent subbands is around $\sim 0,17$ eV. This energy is in good agreement with phonon energy in IR spectra of hBN and BNNTs at 1375 cm^{-1} . From literature it is known that this energy characterizes optical phonons (LO, TO) [54, 55]. PL band 320 nm and its fine structure were observed also by other scientific groups. Under excitation 244 nm this band was found both in hBN, and in BNNTs and BCNNTs [42]. 320 nm band with its characteristic fine structure was observed also in cathodoluminescence spectra [33, 61]. Let us analyse excitation spectra of 320 nm luminescence, seen at Fig. 5.2.2.

This luminescence has several excitation bands. It is excited at 205 nm, corresponding to bound exciton absorption region and at 300 nm with characteristic

fine structure. Separation between adjacent subbands in excitation spectrum is $\sim 0,18$ eV. This means that phonons affect also absorption process and these phonons correspond to optical phonon type (LO, TO) [54, 55]. Fine structure in 300 nm PLE spectrum was observed also in paper [28].

Comparing position of 320 nm luminescence and 300 nm excitation band (Fig. 5.2.2) it is seen that these bands overlap. The 305 nm subband is mutual for luminescence and excitation bands (though small). This can speak in favour of zero phonon line presence. Partial overlapping of PL and PLE spectra is characteristic for the processes where absorption and emission occurs inside one and the same atom. The observed properties allow concluding that the main part of 320 nm luminescence belongs to intracenter process, occurring inside one defect. It does not exclude possibility of ionizing of luminescence center and presence of recombination process.

The mentioned properties of PL and PLE are observed in all samples (A, B, C, D), regardless material size.

Assumption about intracenter origin of 320 nm luminescence allows reasonable explanation of the observed thermal evolution of its intensity in broad temperature range 300 - 8 K. 320 nm luminescence measurements show that luminescence intensity grows at low temperatures (Fig. 5.2.4).

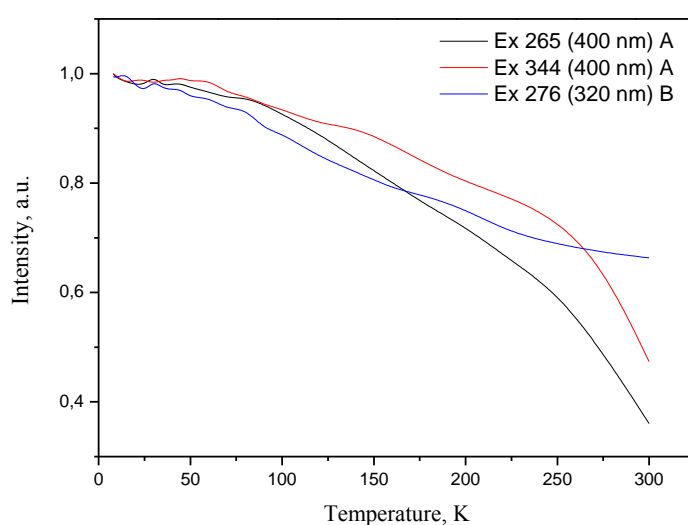


Fig. 5.2.4 Thermal evolution of 320 nm and 400 nm PL bands' intensity at different excitations for hBN macromaterial (samples A, B). Luminescence (in brackets) and excitation wavelengths are shown at the right.

Change of 320 nm PL band intensity at different temperatures may be explained by using schematic depiction of an atom ground and excited states in terms of configuration coordinates (Fig. 5.2.5).

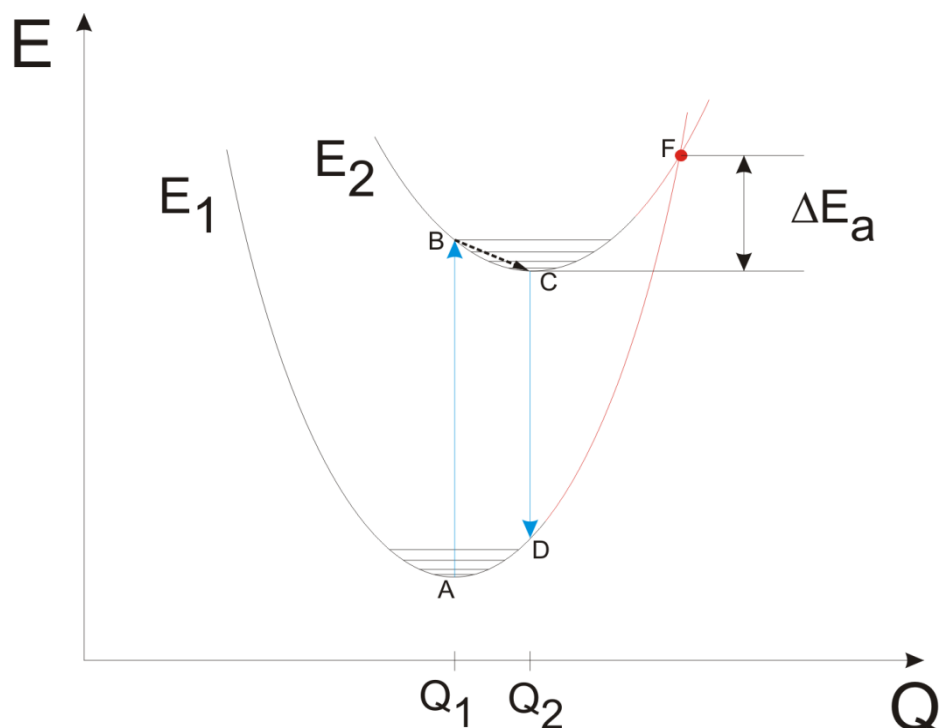


Fig. 5.2.5 Schematic depiction of an atom ground and excited states in energy and configuration coordinates.

The excited luminescence centre/atom according to Fig. 5.2.5 corresponds to point B: there are several ways how it can return to the ground state: 1) relaxing and transferring the excess energy to crystal lattice ($B \rightarrow C$) it emits light quantum ($C \rightarrow D$); 2) using phonon energy it overcomes energy barrier ΔE_a and by radiationless process comes to the ground state u ($C \rightarrow F \rightarrow A$); 3) using phonon energy the excited atom can be ionized with an electron transfer to the conduction band. (This case does not belong to the intracenter process and is not shown in Fig. 5.2.5). With temperature drop phonon energy is becoming lower and number of radiationless transitions is reduced, probability of the second and third processes decreases. As a result a number of optical transitions followed by light quantum emission increases, that causes intensification of luminescence.

The 320 nm luminescence process can be estimated by analysing its kinetics. Luminescence decay pulse consists mainly of a fast component, which decay time is around 4ns. The fast component is dominating. The 320 nm band is characterized with fast processes, which could describe intracenter processes. Luminescence decay slow component is negligible small. Correspondence of the 320 nm band to the fast processes is confirmed also by the luminescence spectrum measured in the pulsed mode (sample A, 300 K), when only a fast part of a pulse (<10 ns) is detected (Fig. 5.2.6). The obtained spectrum is in good agreement with the 320 nm band.

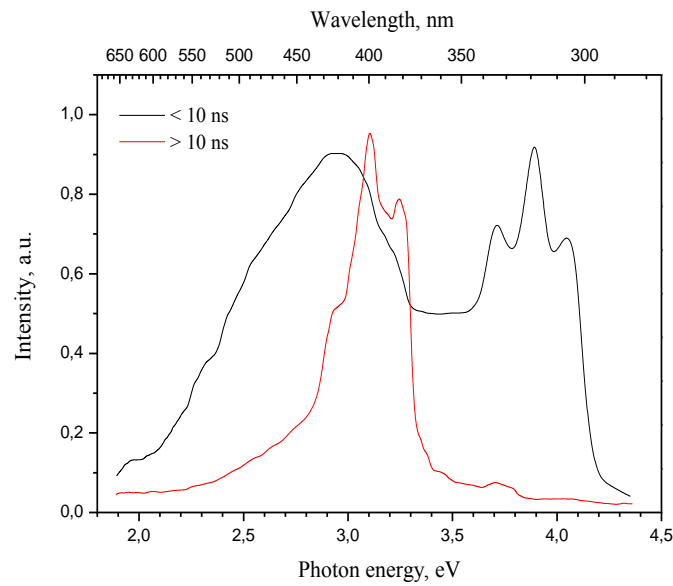


Fig. 5.2.6 PL spectra of hBN macromaterial (sample A) at 300 K. Luminescence is excited in pulse mode. Black curve – luminescence spectrum for pulses < 10 ns (a fast decay component); red curve – luminescence spectrum for pulses > 10 ns.

Luminescence kinetics was studied also in Wu paper [34]. The obtained results are in good agreement with the above mentioned.

Participation of 320 nm luminescence centres in recombination processes may be estimated by studies of stimulation luminescence of the samples previously irradiated with UV light.

320 nm luminescence band is seen also in TL emission spectrum (Fig. 5.2.7). Two thermal peaks correspond to 320 nm luminescence on TL glow curve of hBN - those at 80 °C and 360 °C, while the third peak at 520 °C appears on the TL glow curve of BNNTs.

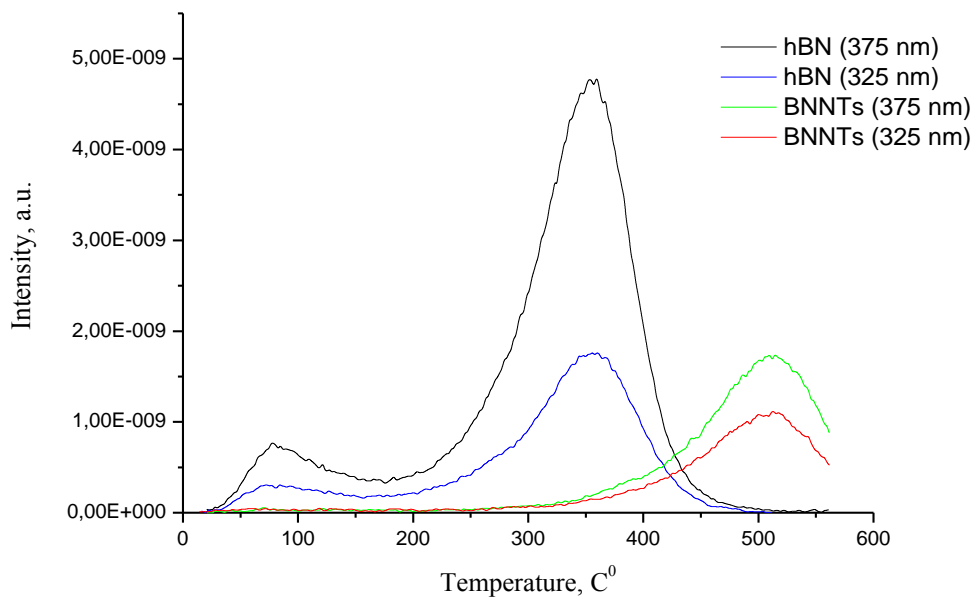


Fig. 5.2.7 Thermoluminescence glow curves of hBN (sample A) and BNNTs (sample C) corresponding to emission intervals around 375 nm and 325 nm.

It means that irradiation of material with UV light causes energy storage and recombination processes with participation of a shallow (releasing at $T \approx 80^\circ\text{C}$) and two deep (360 and 520°C) trapping centers of free charge carriers. However, we can not eliminate possibility that TL curves are produced by other luminescence centres, whose emission overlaps with 320 nm region, because TL curves were measured selecting luminescence with optical glass filters. In OSL emission spectra (Fig.5.2.8) 320 nm band is not observed, it may be explained by low intensity of recombination luminescence.

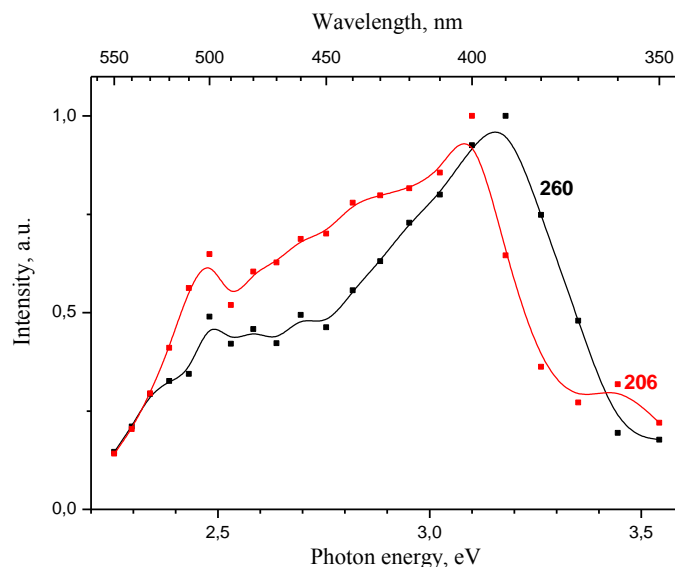


Fig. 5.2.8 OSL emission spectra of hBN macromaterial (sample A) at 300 K. Wavelengths (in nm) of preliminary irradiation are shown near curves.

Studies of luminescence spectra and kinetics allow concluding that in hBN and BNNTs the main contribution to 320 nm luminescence is given by intracenter processes and the smaller part is due to recombination processes.

In order to estimate location of luminescence centres in crystal lattice dependence of 320 nm band on ambient atmosphere was studied for hBN and BNNTs. It was observed that intensity of 320 nm band is not affected by atmosphere (vacuum, air, O₂, N₂, Ar gases) surrounding sample. (Fig.5.2.9). It could imply that this luminescence is connected not with surface defects but with defects in bulk of material [65].

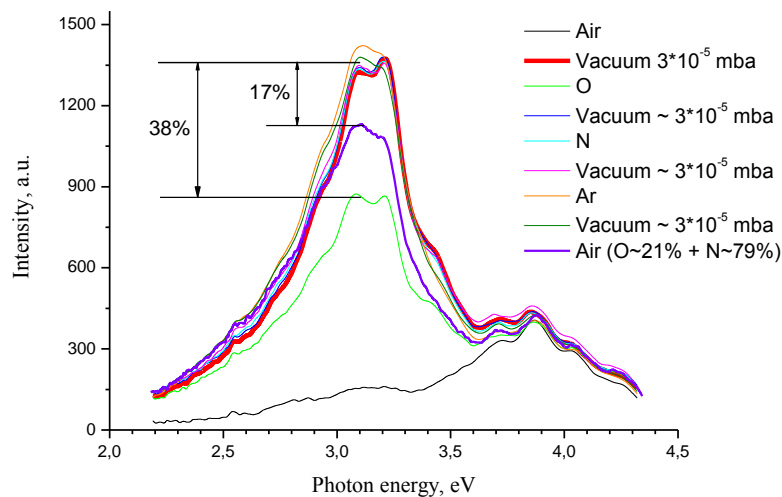
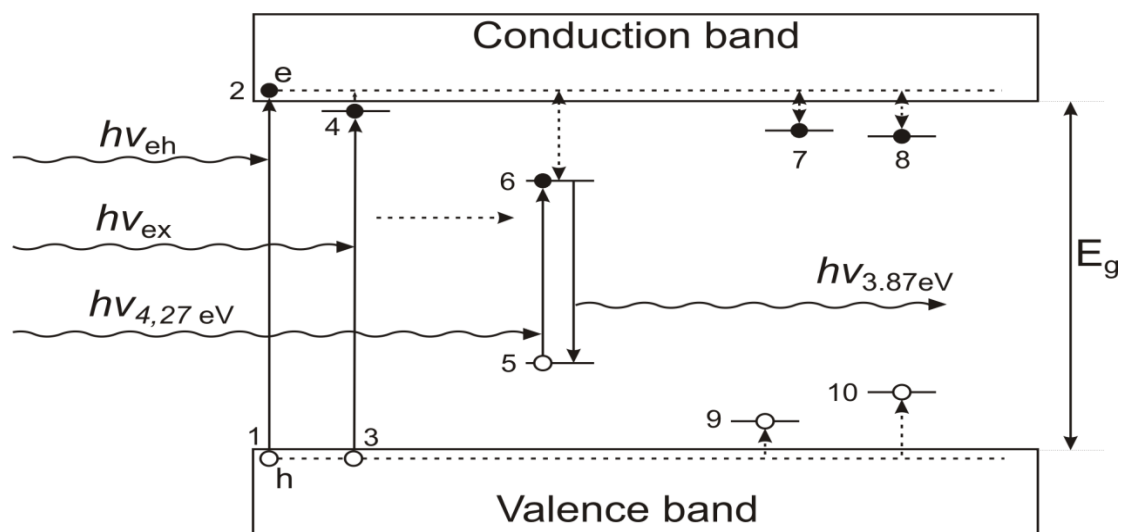


Fig. 5.2.9 PL spectrum of hBN macromaterial (sample A) excited by 270 nm light, sample inserted in different atmospheres: air, vacuum and O, N, Ar gases.

The obtained results together with literature data allow proposing luminescence mechanism of 320 nm band, which is schematically shown in energy band diagram in Fig. 5.2.10.



5.2.10 Fig. hBN energy band diagram illustrating the model of 320 nm luminescence.

The possible luminescence processes connected with 320 nm emission band are considered in terms of energy band diagram. Fig. 5.2.10 shows valence and conduction bands, band gap with width E_g , band-to-band transition (1 – 2), exciton state (3,4), ground state (5) and excited state (6) of luminescence centre, electron trapping centres (7,8) and hole trapping centres (9,10). Besides, there are shown quanta of excitation light corresponding to band-to-band excitation $h\nu_{eh}$, exciton excitation $h\nu_{ex}$, and defect excitation $h\nu_{4,27eV}$, as well as luminescence quantum $h\nu_{3,87eV}$. Band-to-band transition (1-2) can cause host lattice luminescence (2-1) and generation of an exciton. Electrons/holes moving along their energy bands can be captured by corresponding trapping centres (7, 8/9, 10). Stimulation energy in the form of light or heat releases electrons/holes from trapping centres, they return to conduction/valence band and can participate in further processes, particularly interact with a luminescence centre. In the investigated hBN this process is possible because 320 nm luminescence is revealed in TL emission spectra. Excitation of excitons (transition 3-4) can cause exciton luminescence (4-3), exciton dissociation to an electron and a hole, exciton localisation near a defect generating a bound exciton, which can raise its own luminescence or transfer its energy to defects, which in their turn will be excited and give luminescence. This process occurs in hBN, because 320 nm luminescence is excited in the free and bound exciton absorption bands. 320 nm luminescence can be excited directly in the defect absorption band 300 nm (4,27 eV), corresponding to transition (5-6), from where electron returning to the ground state (6-5) is followed by 320 nm luminescence. Ionisation of the defect in the excited state is characterised with low probability, because no 320 nm band was observed in OSL emission spectrum. However, TL measurements have shown presence of 320 nm luminescence. Presence of recombination process is implied also by shape of 320 nm photoluminescence pulse, where besides the main part consisting of short component, corresponding to intracenter process, there is also a slow component characteristic to recombination process.

Analysis of the above mentioned spectral results allow the following conclusions:

- Both boron nitride (hBN) macrosized material and nanotubes (BNNTs) reveal 320 nm luminescence originating from natural impurity point defect. This luminescence occurs mainly due to intracenter processes, where a luminescence centre – impurity ion is excited directly by a light quantum corresponding to its absorption band (300 nm), or through energy transfer from an exciton. Excitation is followed by light emission, producing light quantum 320 nm.

Regrettably, the used spectral and X ray methods do not allow identification of origin of natural point defects, responsible for 320 nm luminescence. This problem was discussed in papers of other authors [32, 33, 42, 61]. As the most probable candidates for this luminescence centre there were mentioned C or O atoms, substituting for N in BN crystal lattice. It was found that increase of C and O concentration causes growth of 320 nm luminescence intensity [33]. EPR method [23] also was tried but it did not give an unambiguous answer.

b) 400 nm luminescence

Let us analyse properties of the 400 nm band.

A broad 400 nm (3,1 eV) PL band with its characteristic fine structure has been observed in all studied samples A, B, C, D at room and low temperatures (see Fig. 5.2.1). This band has subbands at 380 nm (3,26 eV), 400 nm (3,1 eV), 420 nm (2,95 eV). Separation distance between adjacent subbands is around $\sim 0,16$ eV. According to IR absorption measurements this energy corresponds to energy of optical phonons (LO, TO) similarly to the case 320 nm band.

The 400 nm luminescence band is excited both in two defect absorption bands (265 nm and 340 nm) and due to energy transfer from excitons (Fig. 5.2.11).

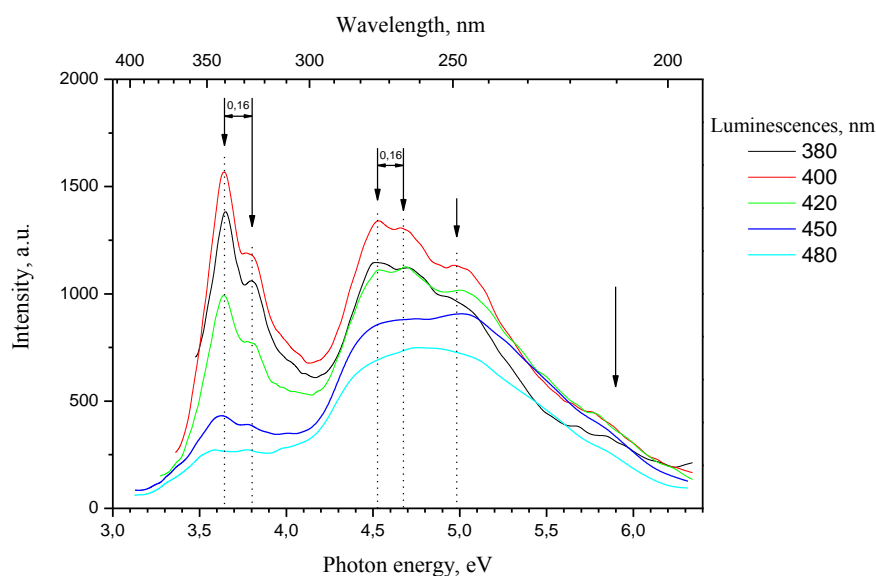


Fig.5.2.11 PLE of hBN macromaterial (sample A) at 8 K. Selected luminescence wavelengths are seen at the right.

Excitation spectra of 400 nm luminescence of hBN and BNNTs has three bands at 205 nm, 265 nm, and 340 nm. 205 nm band corresponds to excitation of excitons, but 265 nm and 340 nm bands correspond to defect absorption. Both defect absorption bands are characterised with fine structure, which is worse pronounced in case of nanomaterial. It may be explained by use of widely open monochromator slits because of low intensity of nanomaterial luminescence. Separation distance between adjacent subbands in excitation spectrum is ~ 0.20 eV, this energy corresponds to optical phonons (TO). Presence of fine structure in these spectra testifies influence of phonons on absorption processes. Presence of two different bands corresponding to defect absorption allows concluding that 400 nm luminescence centre has at least two levels of excited state.

The results obtained allow concluding that 400 nm luminescence in hBN and BNNTs can be caused by direct excitation of defect centre or by energy transfer from excitons [our papers 30, 61].

Studying dependence of 400 nm luminescence intensity on temperature $I=f(T)$ in thermal region 300 K - 8 K under 265 nm and 340 nm excitation it was found that decrease of temperature causes growth of 400 nm luminescence intensity (see Fig.5.2.4). The corresponding curves characterising this process have a turning point at around ~ 220 K, in lower temperature region luminescence intensity changes faster, than in higher temperature region. It could be explained by assumption that two different processes each with its own thermal dependence, contribute to 400 nm luminescence. They can be intracenter and recombination processes. In both thermal regions both processes are active, but their contribution is different. The intracenter processes can be explained similarly to the case of 320 nm luminescence (Fig. 5.2.5) with the difference that 400 nm luminescence is due to luminescence centre with two excited states, between which radiationless transitions occur. In case of recombination process the luminescence defect – impurity atom interacts with other close defect – an electron trapping centre, forming a defect pair (AD pair). In this process an excited defect/atom ionizes, the released electron is captured by a close trapping centre, and then follows recombination with an ionized atom and emission of 400 nm light quantum.

Studies of luminescence kinetics confirm presence of two different luminescence mechanisms in 400 nm luminescence. 400 nm luminescence pulse comprises a fast component and a slow component. Similarly to 320 nm luminescence case, also 400 nm luminescence decay fast component may be exponentially approximated obtaining life time faster than 5 ns. The pulse fast component characterises intracenter luminescence. The fast component intensity of the 400 nm band gives only small contribution to the total pulse intensity, the main contribution given by the slow component. The slow component of the pulse most probably characterizes the recombination part of luminescence. The slow component cannot be approximated by a single exponent; this confirms that processes are complicated and imply participation of several different trapping centres. (Difference can be both in type of trapping centres and their location in relation to a luminescence centre.) The dominating role of the slow component of the 400 nm luminescence pulse is confirmed also by luminescence spectrum (Fig. 5.2.6), which is obtained only for the pulse slow component, the fast components being cut off. This spectrum well describes 400 nm luminescence band and its fine structure. The mentioned above facts imply that 400 nm luminescence is caused mainly by recombination processes with participation of several different trapping centres, which form pairs with luminescent atoms.

Correspondence of the 400 nm emission band to recombination processes in hBN and BNNTs material is confirmed by OSL and TL measurements (Fig.5.2.7 and 5.2.8). TL measurements confirm presence of at least three trapping centers with different energy depths. In macromaterial it was observed that energy is released at two temperatures - 80°C and 360°C , testifying presence of a shallow and a deep trapping level in energy band gap. In nanomaterials energy is released also at $\sim 520^{\circ}\text{C}$, which means that there is one more ever deeper trapping level in band gap.

In OSL emission spectrum the 400 nm band is well pronounced (Fig., 6.6.1), and even dominating in this spectrum.

The mentioned above results allow concluding that in all studied boron nitride materials, including macrosized powders and multiwall nanotubes, the 400 nm luminescence band is caused mainly by recombination processes, and a small contribution comes from intracenter processes.

The results obtained allow proposing a model of 400 nm luminescence, describing luminescence mechanisms in hBN and BNNTs materials and explaining the known experimental results.

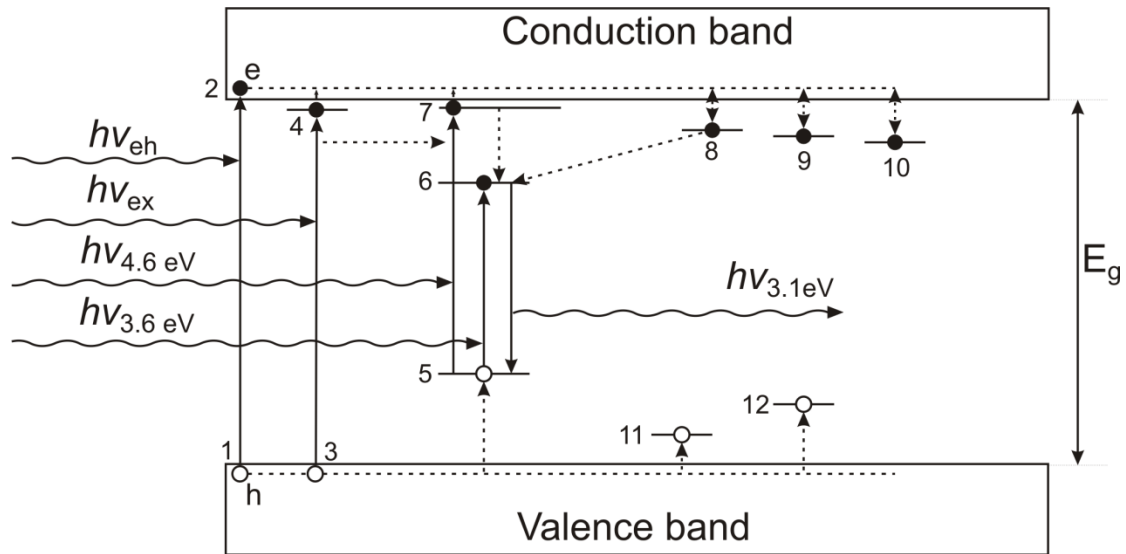


Fig.5.2.12 hBN energy band diagram illustrating the model of 400 nm luminescence.

A model of the 400 nm band is illustrated by the energy diagram of boron nitride (Fig. 5.2.10), which shows valence and conduction bands, band gap with width E_g , exciton state (3,4), energy levels of natural defect-induced energy levels: ground state (5), the first excited state (6) and second excited state (7), electron trapping centres (8, 9, 10) and hole trapping centres (11, 12). A defect (5) together with a close electron trapping centre (8) forms a defect pair (DA pair). Besides, there are shown quanta of excitation light corresponding to band-to-band excitation $h\nu_{eh}$, exciton excitation $h\nu_{ex}$, and two different defect excitations $h\nu_{3,6\text{ eV}}$ and $h\nu_{4,6\text{ eV}}$. Also luminescence quantum $h\nu_{3,1\text{ eV}}$ is shown, emitted by impurity atom passing from excited state 6 to the ground state 5. Excitation of band-to-band transition (1-2) generates an electron (e) in the conduction band and a hole (h) in the valence band. Excitation of an exciton with light quantum $h\nu_{ex}$ causes exciton luminescence or energy transfer to defects in host lattice, among them to a defect (5), producing its excitation (states 6,7). This process is also observed in the investigated materials, because 400 nm luminescence is excited in exciton absorption band.

400 nm luminescence can be excited directly in the defect absorption band 340 nm (3,6 eV), corresponding to transition between energy levels 5-6 and in defect absorption band 265 nm (4,6 eV), corresponding to transition 5-7. Luminescence $h\nu_{3,1\text{ eV}}$ corresponds to transition between levels 6-5. No luminescence bands corresponding to transitions 7-5 and 7-6 were observed experimentally. It allows

concluding that excitation of the impurity centre to the highest energy level will cause the following processes. 1) In radiationless way, transferring the excess energy to lattice vibrations, an excited atom (7) passes to the lowest excited state (level 6) and emits 400 nm luminescence (transition 6-5). This process together with the direct excitation of the transition 5-6 characterises intracenter luminescence. 2) In the highest excited state an atom can ionize, an electron passing either to the close trapping centre (8) or to the conduction band. Similar ionization process of impurity atom is possible when it is in the lower excited state (6). If an ionized impurity centre together with an electron trapped defect forms a pair of close defects, then there follows recombination process causing emission of 400 nm luminescence. (Similar process has been found in case of AlN, where 420 nm luminescence is caused by recombination between close defects – oxygen atom substituting for nitrogen O_N and aluminium vacancy V_{Al} [64]).

If an electron from an ionized impurity centre passes to the conduction band, it can be trapped by different trapping centres (9, 10), which form energy levels of different deepness below conduction band and are not located close to an impurity atom (5). Optically or thermally released from these trapping centres (9, 10) electrons can move through the conduction band and recombine with the existing hole centres, including ionized impurity centres, causing their luminescence (OSL and TL).

In order to determine location of 400 nm luminescence centres in crystalline lattice we have studied dependence of 400 nm band on effect of the ambient conditions, the samples being inserted in vacuum, air, as well as different gaseous (oxygen, nitrogen, argon) atmospheres (Fig. 5.2.9). It was found that 400 nm band's intensity is affected by presence of air and oxygen. Intensity of 400 nm band is ~ 8 times higher for a sample in vacuum than that in air. For sample inserted in oxygen atmosphere decrease of 400 nm luminescence intensity constitutes 38% for hBN and 35% for BNNTs, compared to that in vacuum. However, when camera was filled with ambient air (O ~21 % and N ~ 79%) the 400 nm luminescence decreased by 17 % , but after air pumping out it did not reach the previous level in vacuum as it was in the case of pure oxygen. To the contrast, when the sample is put into nitrogen or argon atmosphere intensity of the 400 nm band does not change compared to that in vacuum. This experiment implies that presence of ambient oxygen quenches 400 nm luminescence, that is decreases the number of luminescence centres, responsible for 400 nm band. This means that 400 nm band could be associated with defects located on material surface or near it [65]. One of such defects could be a nitrogen vacancy V_N on material surface; this assumption is in good agreement with theoretical work [51] showing that oxygen interacts with V_N decreasing its concentration.

The above mentioned effect could be applied for detection of oxygen in the ambient atmosphere (oxygen sensor). For this reason repeatability of the above mentioned measurements was studied. Experiment was run in several cycles. In each cycle 400 nm luminescence was measured first in vacuum and then in oxygen atmosphere. It was found a good repeatability – in ten cycles only very small changes in luminescence intensity were observed. These results allow proposing hBN material for application as oxygen sensor.

The above mentioned analysis of spectral studies allows concluding the following:

- hBN and BNNTs are characterised with 400 nm luminescence caused by natural impurity defects located either on the material surface or in its vicinity. Luminescence centre is formed by closely located defects pairs, consisting of an impurity atom and an electron trapping centre. This luminescence is mainly caused by recombination processes in these defect pairs centres followed by an impurity atom. Besides, there are possible also intracenter processes in an impurity atom without participation of a trapping centre. If electrons from ionized impurity atom are captured by energetically deeper and farther located trapping centres, then there occurs storage of energy, which can be released by thermal or optical stimulation producing thermoluminescence or optically stimulated luminescence, correspondingly.

Regretfully, the present results do not allow identifying of the luminescence centre and corresponding defects. According to the above mentioned it is a defect pair consisting of luminescent impurity atom and a close electron trapping centre. In literature natural luminescent impurities usually are associated with C or O atoms [33, 42, 61] substituting for N atom (C_N or O_N) in hBN crystal lattice. Nitrogen vacancy v_N may be mentioned as potential electron trapping centre. This assumption also explains decrease of 400 nm luminescence intensity when a sample is inserted in oxygen atmosphere, because it is known [51] that v_N binds up oxygen.

c) PL bands in 500 nm region

In hBN and BNNTs materials there are several PL bands observed in the 500 nm region (Fig.5.2.13); they are described in our paper [63].

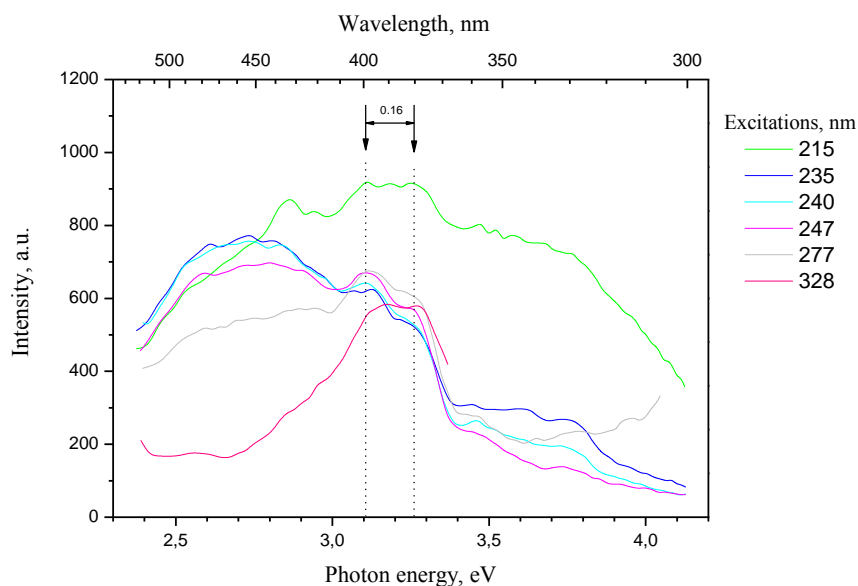


Fig.5.2.13 PL spectra of BNNTs nanomaterials (sample D) at temperature 8 K. Excitation wavelengths are shown at the right.

The bands are broad and evidently contain several subbands, which can be caused by different defects. Excitation for this luminescence is located mainly at

240 nm but smaller excitation bands are observed also at 265 nm and 340 nm (Fig. 5.2.14).

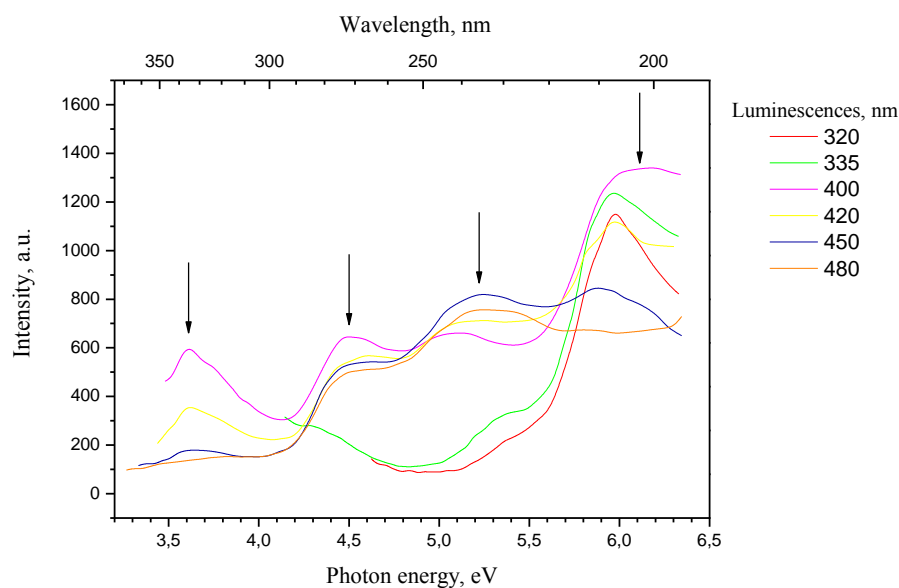


Fig. 5.2.14 PLE spectra of BNNTs nanomaterials (sample D) at temperature 8 K. Selected luminescence wavelengths are shown at the right.

Two latter bands correspond to direct excitation of 400 nm luminescence, therefore it may be concluded that there occurs energy transfer between defects, responsible for 400 nm and 500 nm luminescence.

In BNNTs material there are observed several PL bands in the 500 nm region, whose origin is not known. One of them could be ZrO_2 luminescence at 480 nm [64], because XRD and XRF studies have shown presence of ZrO_2 and Zr impurities in this sample.

At present origin of the observed 440 nm luminescence band in BNNTs is not identified. Possibly it is associated with some impurity defects.

6. Conclusions

1. Photoluminescence spectra caused by natural defects in all studied materials - two hBN macrosized powders and two multiwall nanotube samples – are very similar. The most intensive bands are observed at 320 nm and 400 nm. Ratio of the above mentioned bands can vary, but their spectral position remains constant in different boron nitride materials. The observed facts allow concluding that the same defects, which are generated in BN crystal lattice during synthesis, are characteristic both to macromaterial and nanomaterial; they are not affected by material size.
2. In all studied BN materials fine structure is observed for both 320 nm and 400 nm luminescence bands and their excitation bands, corresponding to defect absorption. Separation energy between adjacent subbands does not exceed 160 meV – 200 meV value. Infrared light absorption studies fulfilled in these materials allow concluding that fine structure observed in luminescence and absorption spectra is caused by optical phonons (LO and TO).
3. In hBN and BNNTs materials 320 nm and 400 nm luminescence is excited both in absorption bands of the corresponding defects and by sample irradiation with UV light from free and bound exciton absorption region. It allows concluding that in BN material excitons transfer their energy to defect centres causing their luminescence.
4. The fulfilled spectral measurements allow proposing luminescence mechanism for 320 nm band in hBN and BNNTs. Basing on the experimental results it is concluded that the main contribution to 320 nm luminescence is done by intracenter processes, where light absorption and emission occurs in one and the same impurity atom and emission follows absorption. It is confirmed by the following facts: *i*) luminescence band and its excitation bands are located very close and even partially overlap, *ii*) luminescence decay pulse is formed mainly by a fast component, which is characteristic for intracenter processes *iii*) 320 nm luminescence band is not observed in OSL emission spectra.
Regrettably, the obtained results are not sufficient for identification of the luminescence centre. Investigations of other researchers allow assenting to their assumption that 320 nm luminescence could be caused by C or O impurities.
5. 320 nm luminescence is insensitive to the sample ambient atmosphere – oxygen, nitrogen or argon gases. It allows concluding that the above mentioned gases do not interact with the 320 nm luminescence centres, and they probably are located in bulk of BN crystalline lattice.
6. The fulfilled studies in hBN and BNNTs allow proposing mechanism of 400 nm luminescence. The obtained results confirm that the main contribution in 400 nm luminescence is given by recombination processes that means that close

point defect pairs are involved in luminescence process. Recombination nature of 400 nm luminescence is proved by the following facts: *i)* luminescence decay pulse comprises fast and slow components; among them dominates the slow component, characterising recombination process. This slow component cannot be approximated by a single exponent, this implies presence of several charge carrier trapping centres participating in the recombination process. *ii)* 400 nm luminescence is observed in OSL and TL processes. A part of 400 nm luminescence is caused by intracenter processes. It is proved by presence of fast component in the luminescence decay pulse.

7. The present data do not allow identification of defects responsible for 400 nm luminescence in hBN and BNNTs. However the weight of evidence suggests that the corresponding defects are located on material surface or in its vicinity. This is testified by dependence of 400 nm luminescence intensity on amount of oxygen in ambient atmosphere.
8. The observed dependence of 400 nm luminescence intensity on amount of oxygen in ambient atmosphere in hBN and BNNTs and good repeatability of measurements allow proposing this material for application in oxygen sensors.

7. Thesis

1. hBN and BNNTs are characterised with 400 nm luminescence caused by natural impurity defects, which are located on material surface or in its vicinity. Luminescence centre is formed by a pair of close defects, comprised of a luminescent impurity atom and an electron trapping centre. Impurity atom can be excited either directly (two excitation/absorption bands at 265 nm and 340 nm), or receiving energy from excitons. Excitation is followed by 400 nm emission. A small part of this luminescence is determined by intracenter processes in an impurity atom, while the main part is formed by the recombination processes between defects in close pairs.
2. In hBN and BNNTs there is observed the dependence of 400 nm luminescence intensity on amount of oxygen in ambient atmosphere, which allow proposing this material for potential application in oxygen sensors.

8. References

- [1] J. Huang and Y. T. Zhu, Defect and Diffusion Forum vols, **186-187**, (2000), p. 1-32.
- [2] M. Ishigami, S. Aloni and A. Zettl, AIP Conference Proceedings, (2003), p. 94-99.
- [3] W. H. Balmain, Journal of Praktical Chemistry, **27**, (1842), p. 422-430.
- [4] J. Thomas, N. E. Weston, T. E. O'Connor, J. Am. Chem. Soc., **84**, (1962), p. 4619-4622.
- [5] X. Hao, M. Yu, D. Cui, X. Xu, Q. Wang and M. Jiang, Journal of Crystal Growth, **241**, (2002), p. 124-128.
- [6] X. Hao, Y. Wu, J. Zhan, X. Xu, M. Jiang, Crystal Research and Technology, **40**, (2005), p. 654-657.
- [7] L. L. Sartinska, A. A. Frolov, A. Yu. Koval, N. A. Danilenko, I. I. Timofeeva, B. M. Rud, Materials Chemistry and Physics, **109**, (2008), p. 20-25.
- [8] K. Watanabe, T. Taniguchi and H. Kanda, Nature Materials, **3**, (2004), p. 404-409.
- [9] L. Nistor, V. Teodorescu, C. Ghica, J. Van Landuyt, G. Dinca, P. Georgeoni, Diamond and Related Materials, **10**, (2001), p. 1352-1356.
- [10] S. Guerini, P. Piquini, Surface Science, **555**, (2004), p. 179-186.
- [11] N. G. Chopra, R. J. Luyken, K. Cherrey, V. H. Crespi, M. L. Cohen, S. G. Louie, A. Zettl, Science, **269** (1995) p. 966-967.
- [12] Y. Shimizu, Y. Moriyoshi, S. Komatsu, T. Ikegami, T. Ishigaki, T. Sato, Y. Bando, Original Research Article Thin Solid Films, **316**, (1998), p. 178-184.
- [13] Golberg, D. Bando, Y. Eremets, M. Takemura, K. Kurashima and H. Yusa, Appl. Phys. Lett., **69**, (1996), p. 2045 - 2047.
- [14] Y. Chen, J. Fitz Gerald, J. S. Williams and P. Willis, Materials Science Forum Vols, **312-314**, (1999), p. 173-178.
- [15] D. Golberg, Y. Bando, C. Tang, C. Zhi, Advanced Materials, **19**, (2007), p. 2413-2432.
- [16] X. Blase, A. Rubio, S. G. Louie and M. L. Cohen, Europhys. Lett., **28**, (1994), p. 335-340.
- [17] J. S. Lauret, R. Arenal, F. Ducastelle, and A. Loiseau, M. Cau, B. Attal-Tretout, and E. Rosencher, L. Goux-Capes, Phys. Rev. Lett., **94**, (2005), p. 037405.
- [18] Y. Chen, J. Zou, S. J. Campbell, G. Le Caer, Appl. Phys. Lett., **84**, (2004), p. 2430-2432.
- [19] C. Zhi, Y. Bando, C. Tang, D. Golberg, Materials Science and Engineering: R: Reports, **70**, (2010), p. 92-111.
- [20] C. Jin, F. L. Kazu, K. Suenaga and S. Iijima, Phys. Rev. Lett., **102**, (2009), p. 195505.
- [21] Y. Miyamoto, A. Rubio, S. Berber, M. Yoon, and D. Tomanek, Phys. Rev. B, (Rapid Communications), **69**, (2004), p. 121413.
- [22] A. Katzir, J. T. Suss, A. Zunger, A. Hampering, Phys. Rev. B, **11**, (1975), p. 2370-2377.
- [23] A. Zunger, A. Katzir, Phys. Rev. B, **11**, (1975), p. 2378-2390.
- [24] E. Y. Andrei, A. Katzir, and J. T. Suss, Phys. Rev. B, **13**, (1976), p. 2831-2834.
- [25] У. Д. ДЖУЗЕЕВ П.Е. РАМАЗАНОВ, СПЕКТРЫ ФОТОЛЮМИНЕСЦЕЦИИ НИТРИДА БОРА АКТИВИРОВАННОГО НЕКОТОРЫМИ ЭЛЕМЕНТАМИ, ИЗВЕСТИЯ ВЫСШИХ УЧЕБНЫХ ЗАВЕДЕНИЙ, **7**, (1969), P. 81-85.
- [26] O. Tsuda, K. Watanabe, and T. Taniguchi, J. Appl. Phys., **46**, (2007), p. L287-L290.
- [27] K. Watanabe, T. Taniguchi, T. Kuroda, H. Kanda, Diamond and Related Materials, **15**, (2006), p. 1891-1893.
- [28] V. L. Solozhenko, A. G. Lazarenko, J. -P. Petitet, A. V. Kanaev, Journal of Physics and Chemistry of Solids, **62**, (2001) p. 1331-1334.

- [29] O. Tsuda, K. Watanabe and T. Taniguchi, *Diamond and Related Materials*, **19**, (2010), p. 83-90.
- [30] B. Berzina, L. Trinkler, V. Korsak, R. Krutohvastov, D. L. Carroll, K. B. Ucer, and R. T. Williams, *Phys. Stat. Sol. (b)*, **243**, (2006), p. 3840-3845.
- [31] P. Jaffrennou, F. Donatini, J. Barjon, J.-S. Lauret, A. Maguer, B. Attal-Tretout, F. Ducastelle, A. Loiseau, *Chemical Physics Letters*, **442**, (2007), p. 372-375.
- [32] P. Jaffrennou, J. Barjon, J.-S. Lauret, A. Maguer, D. Golberg, B. Attal-Trétout, F. Ducastelle, and A. Loiseau, *Phys. stat. sol. (b)*, **244**, (2007), p. 4147-4151.
- [33] T. Taniguchi, K. Watanabe, *Journal of Crystal Growth*, **303**, (2007), p. 525-529.
- [34] L. Museur, E. Feldbach, A. Kanaev, *Phys. Rev. B*, **78**, (2008), p. 155204
- [35] L. Museur, G. Brasse, A. Pierret, S. Maine, B. Attal-Tretout, F. Ducastelle, A. Loiseau, J. Barjon, K. Watanabe, T. Taniguchi, and A. Kanaev, *Phys. Status Solidi RRL*, **5**, (2011), p. 214-216.
- [36] K. Watanabe, T. Taniguchi, K. Miya, Y. Sato, K. Nakamura, T. Niiyama, M. Taniguchi, *Diamond and Related Materials*, **20**, (2011), p. 849-852.
- [37] K. Watanabe, T. Taniguchi, T. Kuroda, O. Tsuda, H. Kanda, *Diamond and Related Materials*, **17**, (2008), p. 830-832.
- [38] B. Arnaud, S. Lebègue, P. Rabiller and M. Alouani, *Phys. Rev. Lett.*, **96**, (2006) p. 026402.
- [39] L. Wirtz, A. Marini, M. Gruning, A. Rubio, *arXiv:cond-mat/0508421v1*, (2005), p. 1-5.
- [40] L. Wirtz, A. Marini, A. Rubio, *Phys. Rev. Lett.*, **96**, (2006), p. 126104.
- [41] A. Rubio, J. L. Corkill, and M. L. Cohen, *Phys. Rev. B*, **49**, (1994), p. 5081-5084.
- [42] J. Wu, Wei-Qiang Han, W. Walukiewicz, J. W. Ager, W. Shan, E. E. Haller and A. Zettl, *Nano Lett*, **4**, (2004), p. 647-650.
- [43] L. Museura, D. Anglos, J. P. Petitet, J. P. Michel and A. V. Kanaev, *Journal of Luminescence*, **127**, (2007), p. 595-600.
- [44] C. Tang, Y. Bando, C. Zhi and D. Golberg, *Chemical Communications*, (2007), p. 4599-4601.
- [45] B. Berzina, L. Trinkler and K. Atobe, *Phys. stat. sol., (c)*, **1**, (2002), p. 421-424.
- [46] S. Larach and R. E. Shrader, *Phys. Rev.*, **104**, (1956), p. 68-73.
- [47] Valdis Korsaks, *Maģistra darbs*, (2007), p. 1-48.
- [48] H. Chen, Y. Chen, Y. Liu, C.-N. Xu, J. S. Williams, *Optical Materials*, **29**, (2007), p. 1295-1298.
- [49] <http://estudijas.lu.lv/mod/resource/view.php?id=51545>: Mācību materiāls. Kristālu optiskās īpašības. Eksitoni. Ramana izkliede.
- [50] H. Chen, Y. Chen, Y. Liu, *Journal of Alloys and Compounds*, **504**, (2010), p. S353-S355.
- [51] Y. Chen, C.-L. Hu, J.-Q. Li, G.-X. Jia, Y.-F. Zhang, *Chemical Physics Letters*, **449**, (2007), p. 149-154.
- [52] S. Reich and A. C. Ferrari, R. Arenal and A. Loiseau, I. Bello, J. Robertson, *Phys. Rev. B*, **71**, (2005), p. 205201.
- [53] R. J. Nemanich, S. A. Solin, R. M. Martin, *Phys. Rev. B*, **23**, (1981), p. 6348-6356.
- [54] R. Geick, C. H. Perry and G. Rupprecht, *Phys. Rev.* **146**, (1966), p. 543-547.
- [55] J. Serrano, A. Bosak, R. Arenal, M. Krisch, K. Watanabe, T. Taniguchi, H. Kanda, A. Rubio and L. Wirtz, *Phys. Rev. Lett.*, **98**, (2007), p. 095503.
- [56] L. Wirtz and A. Rubio, *Lecture Notes in Nanoscale Science and Technology*, **6**, (2009), p. 105-148.
- [57] V. Pokropivny, S. Kovrygin, V. Gubanov, R. Lohmus, A. Lohmus, U. Vesī, *Physica E: Low-dimensional Systems and Nanostructures*, **40**, (2008), p. 2339-2342.

- [58] Y. Kubota, K. Watanabe, O. Tsuda and T. Taniguchi, *Science*, **317**, (2007), p. 932-934.
- [59] G. Dercz, K. Prusik, L. Pajak, *Journal of Achievements in Materials and Manufacturing Engineering*, **31**, (2008), p. 408-414.
- [60] P. Jaffrennou, J. Barjon, J.-S. Lauret, B. Attal-Trétout, F. Ducastelle and A. Loiseau, *Journal of Applied Physics*, **102**, (2007), p. 116102.
- [61] R. T. Williams, K. B. Ucer, D. L. Carroll. B. Berzina, L. Trinkler, V. Korsak and R. Krutohvastov, *Journal of Nanoscience and Nanotechnology*, **8**, (2008), p. 1-5.
- [62] B. Berzina, L. Trinkler, D. Jakimovica, V. Korsaks, J. Grabis, I. Steins, E. Palcevskis, S. Bellucci, Li-Chyong Chen, S. Chattopadhyay and Kuei-Hsien Chen, *Journal of Nanophotonics*, **3**, (2009), p. 031950.
- [63] V. Korsaks, B. Bērziņa, L. Triklere, *Latvian journal of physics and technical science*, **1**, (2011), p. 55-61.
- [64] K. Smits, L. Grigorjeva, D. Millers, A. Sarakovskis, J. Grabis, W. Lojkowski, *Journal of Luminescence*, **131**, 2011, p. 2058–2062.
- [65] V. Korsaks, B. Bērziņa, L. Triklere. *Latvian journal of physics and technical science*. (Accepted).

9. List of publications

Papers

- 1) B. Berzina, L. Trinkler, V. Korsak, R. Krutohvastov, D. L. Carroll, K. B. Ucer, and R. T. Williams, *Exciton luminescence of boron nitride nanotubes and nano-arches*. Phys. Stat. Sol., (b), **243**, (2006), p. 3840–3845. **SCI**
- 2) R. T. Williams, K. B. Ucer, D.L. Carroll. B. Berzina, L. Trinkler, V. Korsak and R. Krutohvastov, *Photoluminescence of self-trapped exciton in boron nitride nanotubes*, Journal of Nanoscience and Nanotechnology, **8**, (2008), p. 1-5. **SCI**
- 3) V. Korsaks, B. Bērziņa, L. Trinklere, *Low temperature 450 nm luminescence of hexagonal boron nitride*, Latvian journal of physics and technical science, **1**, (2011), p. 55-61. **SCI**
- 4) V. Korsaks, B. Bērziņa, L. Trinklere. *Influence of air, oxygen, nitrogen and argon gases on 400 nm luminescence in hexagonal boron nitride*. Latvian journal of physics and technical science. (Accepted). **SCI**

Conferences

1. V. Korsaks, B. Berzina, L. Trinkler, *Luminiscences procesi h-BN nanostrukturās: nanocaurulēs nanoarkās*, 23. Zinātniskās konferences, veltītas LU profesora Ilmāra Vītola 75 gadu atcerei, Rīga, Latvija, 13 -15. Februāris, 2007.
2. V. Korsaks, L. Trinkler, B. Berzina, Richard Williams, Burak Ucer, David Carroll, *Luminescence of multi-Walled BN nanotubes and its raw material*, Functional Materials and Nanotechnologies, Rīga, Latvija, 1-4 Aprīlis, 2008.
3. B. Berzina, L. Trinkler, V. Korsak, R. T. Williams, K. B. Ucer, D. L. Carroll, *Excitonic and defect luminescence in h-BN powder and BN nanotubes*, Excitonic Processes in Condensed Matter, Kyoto, Japāna, 22-27. Jūnijs, 2008.
4. V. Korsaks, B. Berzina, L. Trinklere, D. Jakimovica, *Fononu struktūra luminescences spektriem heksagonāla bora nitrīda pulverim un nanomateriālam*, 25. Zinātniskā konference, veltīta doc. Ludviga Jansona simtgadei, Rīga, Latvija, 11 – 13. Februāris, 2009.
5. V. Korsaks, B. Berzina, L. Trinkler, R. Williams, B. Ucer, D. Carrol, S. Bellucci and M. Piccinini, *Phonon Structure of Luminescence Spectra of Bulk Hexagonal BN and Multi-Walled BN Nanotubes*, Functional Materials and Nanotechnologies, Rīga, Latvija, 31. Marts – 3. Aprīlis, 2009.
6. V. Korsaks, B. Berzina, L. Trinkler, D. Jakimovica, R. Williams, B. Ucer, D. Carrol, S. Bellucci and M. Piccinini, *Phon Structure of Luminescence and IR Absorption of hBN and BN Nanotubes*, Development in Optics and Communications, Rīga, Latvija, 24 – 26. Aprīlis, 2009.

7. V. Korsaks, B. Berzina, L. Trinkler, R. T. Williams, K. B. Ucer, D. L. Carroll, *Luminescence and its possible mechanisms of bulk h-BN powder and BN nanotubes*, 7th International Conference on Luminescent Detectors and Transformers of Ionizing Radiation, Krakow, Polija, 12 – 17. Jūlijs, 2009.
8. V. Korsaks, B. Berzina, L. Trinklere, *Heksagonālā bora nitrīda luminiscence zemo temperatūru rajonā*, 26. Zinātniskā konference, Rīga, Latvija, 17 – 19. Februāris, 2010.
9. V. Korsaks, B. Berzina, L. Trinkler, *Luminescence of hexagonal boron nitride powder and nanotubes at different temperstures*, Functional Materials and Nanotechnologies, Rīga, Latvija, 16 – 19. Marts, 2010.
10. V. Korsaks, B. Berzina, L. Trinkler, *Lumininescence of hexagonal boron nitride powder and nanotubes at different temperatures and pretreatments*, Europhysical Conference on Defects in Insulating Materials, 2 – 6. Jūlijs, 2010.
11. B. Berzina, V. Korsaks, L. Trinkler, *Excitonic processes and defect luminiscence in bulk h-BN and multiwalled BN nanotubes*, Excitonic and Photonic Processes in Condensed and Nano Materials, Brisben, Austrālija, 11 – 16. Jūlijs, 2010.
12. B. Berzina, V. Korsaks, L. Trinkler, *Native Defect Luminiscence of III Group Element Nitrides AlN and hBN - Bulk and Nanosize*, 9th International Conference on Nitride Semiconductors, Glasgow, Lielbritānija, 10 – 15. Jūlijs, 2011.

Acknowledgements

Special thanks to my scientific supervisor Dr. habil. phys. **Baiba Berzina** for continuous support, provision of information and ideas, as well as discussion of results.

Thanks to my colleague Dr. phys. Laima Trinklere for rendering assistance.

Thanks to my colleagues from ISSP – Linards Skuja, Larisa Grigorjeva, Krisjanis Smits, Anatolijs Sarakovskis, Karlis Kundzins and Alexander Kalinko for assistance in fulfilment of experiments.

Author acknowledges European Union Social Fund for financial support.



LATVIJAS
UNIVERSITĀTE
ANNO 1919

EIROPAS SAVIENĪBA

IEGULDĪJUMS TAVĀ NĀKOTNĒ